Hindawi
International Journal of Aerospace Engineering
Volume 2023, Article ID 6011397, 11 pages
https://doi.org/10.1155/2023/6011397

Research Article

Damage Identification of Rotating Blades Based on Fuzzy C-Means and Frequency Response Function Curvature Methods

Ruize Cui,[1] Zefeng Wang,[2] and Zhiguang Song[1]

[1]*College of Aerospace and Civil Engineering, Harbin Engineering University, Harbin 150001, China*
[2]*Chinese Flight Test Establishment, Xi'an 710089, China*

Correspondence should be addressed to Zhiguang Song; z.g.song@hrbeu.edu.cn

Received 25 December 2022; Revised 9 August 2023; Accepted 18 August 2023; Published 9 September 2023

Academic Editor: Jacopo Serafini

Rotor blades are one of the key components of helicopter. If the blades are damaged, the safety and reliability of the helicopter will be seriously affected. Therefore, it is necessary to investigate the damage identification of the rotating blades. In this paper, a rotating cantilever beam is used to model the rotor blade. Based on the assumed mode method and Hamilton's principle, the equation of motion is formulated, and the correctness of the model is verified by numerical and experimental studies. Altogether, two methods are used to identify the damages on the blade. The first one is the cluster analysis method based on the fuzzy C-mean theory. In order to reduce the dimension of the signal features, the singular value decomposition is introduced. The second method is the curvature of frequency response function method that can be used to determine the exact position of damages. Simulation results show that one can use fuzzy C-mean method to determine whether there is damage on the blade firstly and then determine the exact position of the damage through the curvature of frequency response function method.

1. Introduction

With the development of aerospace science and technology, various types of rotor aircraft gradually have appeared. Their rotor blades will be accompanied by many kinds of problems. As an important part of the rotor type aircraft, it is necessary to monitor and identify the operating state of blades. Serafini et al. [1, 2] presented an original approach to shape-sensing structural health monitoring of helicopter rotors based on strain measurement on the blades both from time and frequency domains. Therefore, the researches on damage identification of this part have gradually become the focus of attention. Under long-term operation in complex working environments of high speed, high strength, and large torque, rotor blades will be affected by wear, cracks, impact, corrosion, etc. Once the blade is damaged by such effects and is not identified at once, it will lead to very serious accidents.

The curvature of frequency response function is one of the important damage identification methods. On the basis of crack detection researches, a new method based on the change of FRF is proposed by Zhou et al. [3]. Manring et al. [4] provided a new method for matching dominant features of frequency response functions (FRFs) and proposed a slicing and shifting method where the key features of a baseline FRF are compared with a similar FRF using cross-correlation and a log-frequency shift (LFS). An upgraded technique based on the finite element approach was proposed by Alshalal et al. [5] for the identification of the extent of the damage for a simply supported steel beam via the frequency response function curvature and its position. Ayisha et al. [6] presented an improved frequency response function curvature method which is both baseline-free and output-only. It employed the cepstrum technique to eliminate decay of higher resonance peaks caused by the temporal spread of real impulse excitation. Sampaio et al. and Maia et al. [7, 8] utilized the FRF curvature method to detect and localize damage in beam-type structures. Instead of relying just on modal information, the method worked over a broadband frequency range

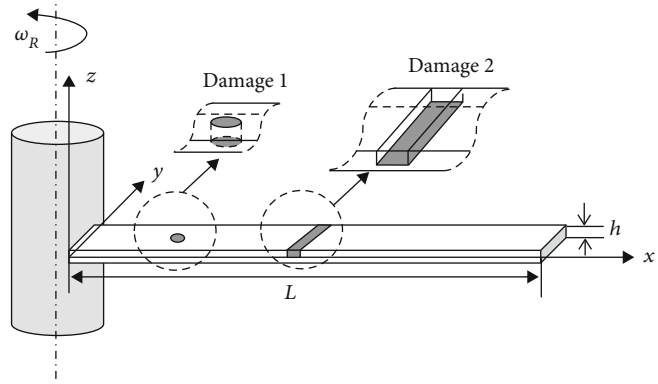

Figure 1: Schematic diagram of the rotating cantilevered beam with damages.

Table 1: Dimensional and nondimensional statistical features and their physical meanings.

Dimensional		Nondimensional	
Expressions	Physical meaning	Expressions	Physical meaning
$\bar{X} = 1/N\sum_{i=1}^{N} x_i$ Mean value	Describe the stability of signals	$S_c = 1/N\sum_{i=1}^{N}\left(\left(x_i - \bar{X}\right)^3/\sigma_x^3\right)$ Skewness	Reflect the asymmetry of signal amplitude
$X_{rms} = \sqrt{1/N\sum_{i=1}^{N} x_i^2}$ Root mean square	Describe the vibration energy of the signal	$K = 1/N\sum_{i=1}^{N}\left(\left(x_i - \bar{X}\right)^4/\sigma_x^4\right)$ Kurtosis	Reflect range of signal impact energy
$\sigma_x^2 = 1/N\sum_{i=1}^{N}\left(x_i - \bar{X}\right)^2$ Variance	Reflect the dynamic part in the change of amplitude	$\mathrm{SH}(x) = \sqrt{N\sum_{t=1}^{N}(x_i)^2}/\sum_{i=1}^{N}\lvert x_i\rvert$ Shape indicator	Reflect the trend of fault signal
$\sigma_x = \sqrt{1/N\sum_{i=1}^{N}\left(x_i - \bar{X}\right)^2}$ Standard deviation	Describe the extent to which data deviate from the mean	$\mathrm{IM}(x) = N\max\lvert x\rvert/\sum_{i=1}^{N}\lvert x_i\rvert$ Impulse indicator	Describe the magnitude of signal impact energy
$X_f = \lvert\max x_i\rvert + \lvert\min x_i\rvert$ Peak-to-peak value	Describes the range of the change of signals	$\mathrm{CR}(x) = \sqrt{N}\max\lvert x\rvert/\sqrt{\sum_{i=1}^{N} x_i^2}$ Crest indicator	Describe the magnitude of signal impact energy
$X_p = E(\max\lvert x_i\rvert)$ Peak value	Describe the strength of the signal	$\mathrm{CL}(x) = N^2\max\lvert x\rvert/\left(\sum_{i=1}^{N}\sqrt{\lvert x_i\rvert}\right)^2$ Clearance indicator	Describe the magnitude change to reflect the wear condition

and proved that curvature-based methods were more efficient than conventional frequency and mode shape-based methods. The main limitation of the FRF curvature method, however, is that its effectiveness is strongly dependent on the frequency range on which it is applied.

In recent years, great progress has been made in damage diagnosis using big data. Fuzzy clustering algorithm is an unsupervised learning method for data classification automatically. It can be used to determine the potential structural information of data and decompose a given set of objects into subgroups or clusters based on similarity. In the cluster analysis, signals belonging to the same cluster are as similar as possible, whereas signals belonging to different clusters are dissimilar. In recent years, the damage identification based on fuzzy clustering attracts the interests of researchers. Palomino et al. [9] proposed a method combining probabilistic neural network and fuzzy cluster analysis methods to identify, locate, and classify two types of damage, namely, cracks and rivet losses in aluminum aircraft window. Ling et al. [10] presented a novel methodology based on fuzzy C-mean (FCM) clustering algorithm and measured FRF data to deal with vibration-based damage detection in a truss bridge model. Liu et al. [11] proposed a two-stage scheme for damage identification using the ratios of modal frequency changes and uniform load surface curvature difference (ULSCD) in damage region. FCM algorithm improved by PSO algorithm (FCM-PSO) was employed to locate damage and predict the damage extent.

Based on the above literature review, it is noted that cluster analysis can make full use of the advantages of big data, and actually, it can be applied in real-time monitoring and damage identification of rotor blades. However, the exact location of damage is not easy to be determined by the cluster method. Therefore, in this study, the combination of the fuzzy C-mean cluster and FRF curvature methods is proposed to investigate the damage identification for rotating blades. In the cluster analysis, singular value decomposition is adopted to reduce the

dimension of the matrix. The theoretical, simulation, and experimental studies are carried out to verify the correctness and effectiveness of the present method.

2. Theoretical Modeling

2.1. Structural Modeling of Rotating Beam. It is noted that rotating beams are widely used in different engineering fields in the forms of wind turbines, airplane rotors, helicopter blades, etc. [12]. Therefore, the rotating Euler-Bernoulli beam [13] is used to simulate the rotating rotor structure. The schematic diagram of the rotating beam is shown in Figure 1. It should be noted that the displacement field, strain-displacement relation, and constitutive equation of any point of the structure are the following [14]:

$$\begin{aligned} u(x,t) &= u_0(x,t) - z\frac{\partial w}{\partial x}, \\ w(x,t) &= w_0(x,t), \\ \varepsilon_x &= \frac{\partial u_0}{\partial x} - z\frac{\partial^2 w}{\partial x^2}, \\ \sigma_x &= E\varepsilon_x, \end{aligned} \tag{1}$$

where u and w are the longitudinal and transverse displacements in the x and z directions, σ_x and ε_x are the stress and strain, and E is the elastic modulus of the material. When the beam rotates around the fixed axis, the centrifugal axial force $F_t(x)$ generated by the rotation can be expressed as

$$F_t(x) = \int_x^L m\omega_R^2 \varsigma d\varsigma = \frac{1}{2}m\left(L^2 - x^2\right)\omega_R^2 = \bar{F}(x)\omega_R^2, \tag{2}$$

where $m = \rho bh$ is the mass of the beam per unit length, in which b is the width, L is the length of the beam along the x direction, and ω_R is the angular velocity of rotation.

The dynamic equation for the rotating beam is established according to Hamilton's principle [15].

$$\int_{t_1}^{t_2} [\delta(T - U) + \delta W]dt = 0, \tag{3}$$

where T and U represent the kinetic energy and potential energy of the beam, respectively, and they can be computed by

$$\begin{aligned} T &= \frac{1}{2}\rho\int_V \left[\dot{u}^2 + \dot{w}^2 + \omega_R^2(x+u)^2\right]\mathrm{d}V, \\ U &= \frac{1}{2}\int_V \sigma_x\varepsilon_x dV + \frac{1}{2}\int_0^L F_t(x)\left(\frac{\partial w}{\partial x}\right)^2 dx, \end{aligned} \tag{4}$$

where ρ is the mass density.

In this study, the assumed mode method [16] is used to discretize the continuous beam structure, and the displacements can be expressed by

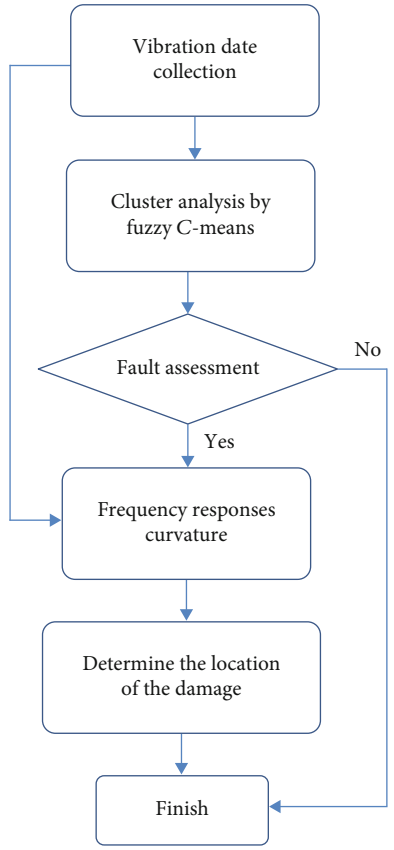

Figure 2: Technical identification process.

$$\begin{aligned} u &= \sum_{i=1}^{n} \psi_i(x)q_i(t) = \psi^T q, \\ w &= \sum_{i=1}^{n} \varphi_i(x)r_i(t) = \varphi^T r, \end{aligned} \tag{5}$$

where ψ and φ are column vectors of mode shapes and q and r are the column vectors of generalized coordinates. For the cantilevered beams, the mode shapes can be assumed as

$$\begin{aligned} \psi_i &= \sin\frac{(2i-1)\pi x}{2L}, \\ \varphi_i &= \cosh\gamma_i x - \cos\gamma_i x - \frac{\cosh\gamma_i L + \cos\gamma_i L}{\sinh\gamma_i L + \sin\gamma_i L}(\sinh\gamma_i x - \sin\gamma_i x), \end{aligned} \tag{6}$$

where γ_i could be obtained from

$$\cos\gamma_i L \cdot \cosh\gamma_i L + 1 = 0, i = 1, 2, \cdots, n. \tag{7}$$

By substituting Equation (5) into Equation (4), and according to the Hamilton principle, the equation of motion of the rotating beam can be obtained:

$$M\ddot{z} + (K_s + K_c - K_r)z = F_0(t)e^{i\omega t}, \tag{8}$$

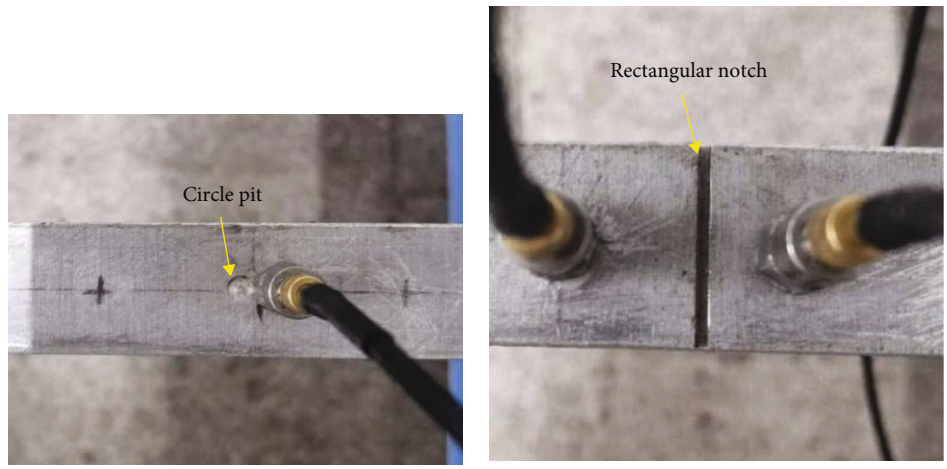

(a) (b)

Figure 3: Two damages on the beam in the experiment: (a) circle pit and (b) rectangular notch.

(a) (b)

Figure 4: Equipment in the experiment: (a) test equipment and (b) specimen.

where $z = [q^T, r^T]^T$, $\boldsymbol{F}_0(t)$ is the external load vector, M is the structural mass matrix, K_s is the structural stiffness matrix, K_c is the stiffness caused by the prestressing due to the inertial force, and K_r is stiffness produced by the rotation softening effect, and they are computed by

$$
\begin{aligned}
M &= \begin{bmatrix} m\int_0^L \psi\psi^T dx & 0 \\ 0 & m\int_0^L \varphi\varphi^T dx + \dfrac{\rho bh^3}{12}\int_0^L \dfrac{\partial\varphi}{\partial x}\dfrac{\partial\varphi^T}{\partial x} dx \end{bmatrix}, \\
K_r &= \begin{bmatrix} \omega_R^2 m\int_0^L \psi\psi^T dx & 0 \\ 0 & \dfrac{\rho bh^3}{12}\omega_R^2\int_0^L \dfrac{\partial\varphi}{\partial x}\dfrac{\partial\varphi^T}{\partial x} dx \end{bmatrix}, \\
K_s &= \begin{bmatrix} Ebh\int_0^L \dfrac{\partial\psi}{\partial x}\dfrac{\partial\psi^T}{\partial x} dx & 0 \\ 0 & \dfrac{Ebh^3}{12}\int_0^L \dfrac{\partial^2\varphi}{\partial x^2}\dfrac{\partial^2\varphi^T}{\partial x^2} dx \end{bmatrix}, \\
K_c &= \begin{bmatrix} 0 & 0 \\ 0 & \dfrac{\omega_R{}^2 m}{2}\int_0^L x^2 \dfrac{\partial\varphi}{\partial x}\dfrac{\partial\varphi^T}{\partial x} dx \end{bmatrix}.
\end{aligned} \tag{9}
$$

The solution of Equation (8) is assumed to be

$$z = z_0 e^{i\omega t}, \tag{10}$$

where $\boldsymbol{z}_0$ is the vibration amplitude. Substituting Equation (10) into Equation (8), one can have

$$z_0 = \left(K_s + K_c - K_r - \omega^2 M\right)^{-1} F_0(t). \tag{11}$$

As a result, the frequency responses can be obtained as

$$
\begin{aligned}
u(x_f, \omega) &= \psi^T(x_f) z_0^u(\omega), \\
w(x_f, \omega) &= \varphi^T(x_f) z_0^w(\omega),
\end{aligned} \tag{12}
$$

where x_f is the location of the response point.

2.2. The Curvature of Frequency Response. The curvature of FRF can be used as the identification parameter [7], from which we can achieve the goal of identifying damage through the change of FRF curvature of damaged and undamaged structures. Therefore, it can be noted that the advantage of the FRF curvature method is that the location of the damage can be determined. However, there must be an undamaged beam that works as the judgment basis, which is the disadvantage of the FRF curvature method.

Table 2: Natural frequencies (Hz) of beams with and without damages obtained by different methods.

	Normal beam			Damaged beam		
	Present	COMSOL	Experiment	Present	COMSOL	Experiment
Mode 1	16.45	16.56	15.63	16.44	16.48	15.63
Mode 2	103.08	103.79	101.60	103.07	102.89	101.30
Mode 3	288.57	290.57	285.90	288.59	290.78	282.90

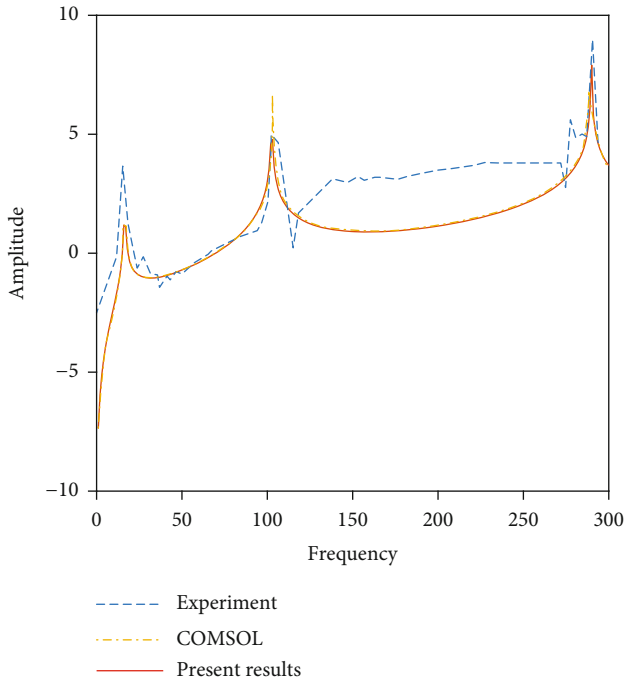

Figure 5: Comparisons of frequency response between different methods.

The curvature of any point on the frequency responses can be calculated by the central difference method as

$$\alpha''(i) = \frac{w(i+1) - 2w(i) + w(i-1)}{d^2}, \tag{13}$$

where d is the distance from the point $i+1$ to the point $i-1$ and $w(i)$ denotes the amplitude of the ith point on the frequency response curve.

Based on the curvature given in Equation (13), a damage index is introduced:

$$\beta = \frac{\left|\alpha'' - \alpha_d''\right|}{\alpha''}, \tag{14}$$

where the subscript "d" denotes the curvature of the damaged structure.

From Equation (14), the location of damage can be identified, i.e., when the structure is damaged, there will be a sudden change in curvature at the damage location.

2.3. Fuzzy C-Means. It can be noted from the above analysis that the curvature of FRF method can easily be used to locate the damage. But the vibration behavior of an identical structure without damage should be known in advance. In addition, the FRF curves are not easy to obtain in the practical working condition. Based on these defects of the FRF curvature method, the present study introduces the fuzzy C-mean method to determine whether the structure is damaged using the time-domain response data. By using such a big data method to process and identify the structural damages [17], it is necessary to redefine the vibration data of many collected signals and analyze whether the data can well reflect the damage from different perspectives. At present, the dimensional and nondimensional definitions of statistical characteristics of time-domain signals that are widely used [18] are given in Table 1.

For the dimensional indicators, they are affected by the working conditions including loads, speeds, and other external conditions. Therefore, there are still certain limitations in practical applications. Dimensionless indicators are evolved from dimensional indicators, which can avoid the influence of these external conditions.

The feature extraction method is the key of the mechanical health monitor and fault diagnosis technology. A good signal process method can extract feature information that will fully express the fault. So firstly, a large eigenvalue matrix is formed by extracting eigenvalues from vibration signals. Due to the huge data, it is necessary to reduce the dimension of the matrix to save the clustering time. In this investigation, the singular value decomposition (SVD) [19] is adopted to reduce the dimension of the matrix. This method basically does not lose the information contained in the matrix, so as to achieve the effect of matrix compression.

Suppose we have n sets of vibration signals $\boldsymbol{x} = [x_1, x_2, \cdots, x_n]^T$, and based on the features given in Table 1, a matrix of feature can be obtained as

$$X = \begin{bmatrix} x_{11} & x_{12} & \cdots & x_{1d} \\ x_{21} & x_{22} & \cdots & x_{2d} \\ \vdots & \vdots & \ddots & \vdots \\ x_{n1} & x_{n1} & \cdots & x_{nd} \end{bmatrix}_{n\times d}, \tag{15}$$

where d is the number of features that are selected from Table 1. Based on the SVD, the matrix X can be expressed as

$$X = U\Sigma V^T, \tag{16}$$

where $U \in \mathbf{R}^{n\times n}$ and $V \in \mathbf{R}^{d\times d}$ are left and right singular vectors and are both orthogonal matrices and $\Sigma \in \mathbf{R}^{n\times d}$ is the

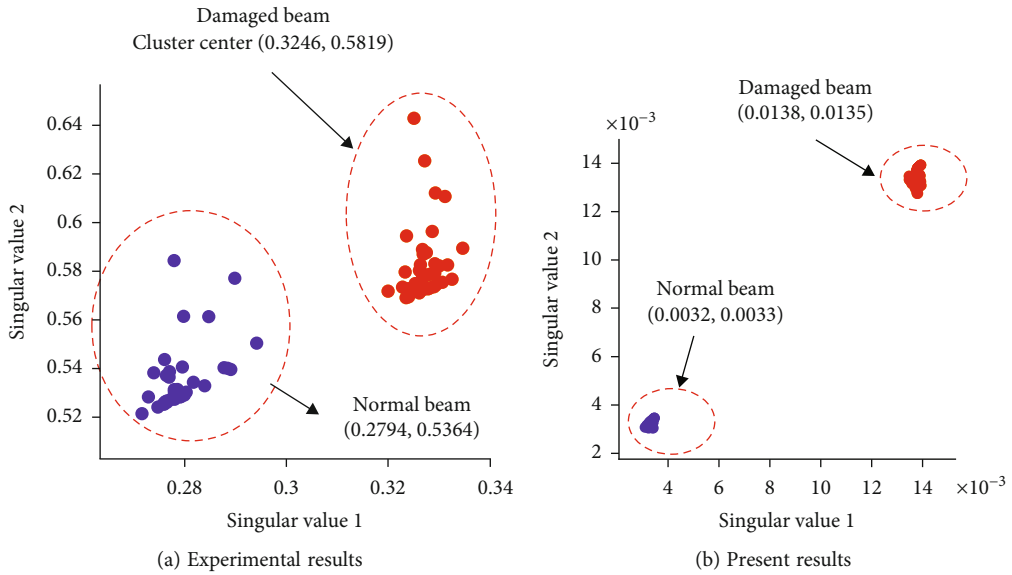

Figure 6: Cluster analysis results of beam without rotation: (a) experimental and (b) theoretical.

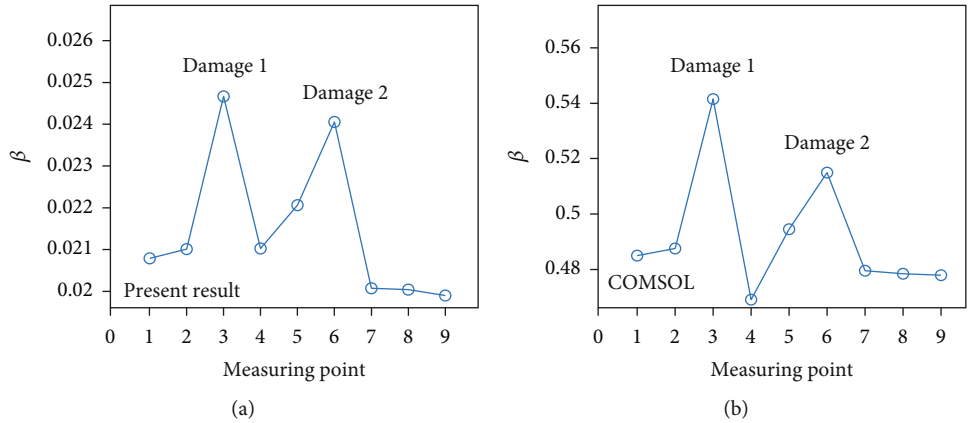

Figure 7: Curvature of frequency response curve by different methods: (a) present result and (b) COMSOL.

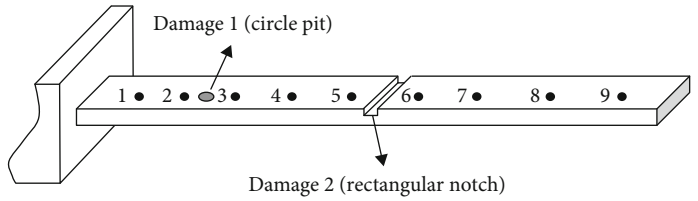

Figure 8: Schematic diagram of beams with damages and measuring points.

singular value matrix whose elements are all zero except for the elements on the principal diagonal. In fact, U and V are eigenvectors of matrices XX^T and X^TX. From Equation (16), one can have

$$X^TX = V\Sigma U^TU\Sigma V^T = V\Sigma^2V^T, \tag{17}$$

from which, the element in the singular value matrix Σ can be obtained as

$$\sigma_i = \sqrt{\lambda_i}, \tag{18}$$

where λ is the eigenvalue of matrix X^TX. It is well known that in matrix Σ, the singular value is arranged from large to small, and the reduction of singular values is particularly fast. In many cases, the sum of the first 10% or even 1% singular values accounts for more than 99% of the sum of all singular values. In other words, we can use the maximum $k\,(k << d)$ singular values and the corresponding left and right singular vectors to approximately describe the matrix X as

$$X \approx U_{n\times k}\Sigma_{k\times k}V^T_{k\times d}, \tag{19}$$

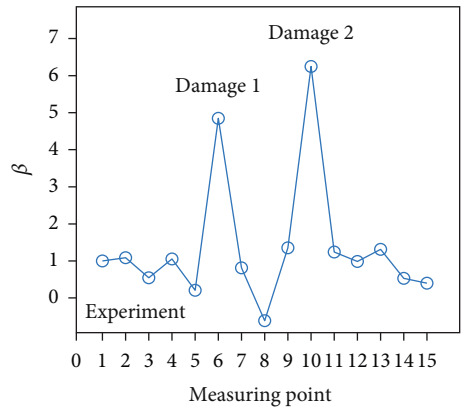

Figure 9: Curvature of frequency response curve obtained by experiment.

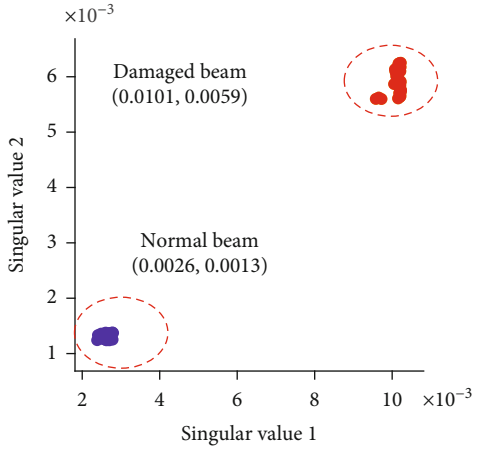

Figure 10: Cluster analysis results for rotating beam.

from which, a compressed matrix can be obtained as

$$\hat{X}_{n\times k} = X_{n\times d} V_{d\times k}. \tag{20}$$

It can be seen from the above equation that the number of columns is compressed. That is to say, the d signal features shown in Table 1 can be compressed to k, where k can be 2. Thus, we can draw the features of each set of vibration signals in a two-dimensional coordinate system.

Next is the clustering analysis based on the fuzzy c-mean method, an algorithm to minimize the objective function [20–22]. The objective function of the FCM is

$$J(u, v) = \sum_{j=1}^{n}\sum_{i=1}^{c} u_{ij}^{m} \left\|\hat{X}_j - v_i\right\|^2, \quad 1 \le m \le \infty, \tag{21}$$

where $\hat{X}_j$ is the jth signal in $\hat{X}$, u is the matrix of degree of membership, $\boldsymbol{v}_i$ is the cluster center, $d_{ij} = \|\hat{X}_j - v_i\|^2$ is the Euclidean distance between the ith cluster center and the jth data point, and m is the weighted index whose experience range is from 1.1 to 5 [23, 24].

Table 3: Natural frequencies (Hz) of rotating beam with damages obtained by different methods.

	Present results	COMSOL
Mode 1	23.866	23.951
Mode 2	110.74	110.68
Mode 3	296.28	298.21

For the matrix of degree of membership, its form is

$$u = \begin{bmatrix} u_{11} & u_{12} & \cdots & u_{1k} \\ u_{21} & u_{22} & \cdots & u_{2k} \\ \vdots & \vdots & \ddots & \vdots \\ u_{n1} & u_{n2} & \cdots & u_{nk} \end{bmatrix}, \tag{22}$$

in which,

$$\forall i, \sum_{j=1}^{c} u_{ij} = 1; \forall i, j, u_{ij} \in [0, 1], \tag{23}$$

which indicates that each cluster, the summation of the degrees of membership is 1 [25].

In order to obtain $\boldsymbol{u}$ and $\boldsymbol{v}_i$, a Lagrange function is constructed by introducing a Lagrange multiplier as [26, 27]

$$L(u, v) = \sum_{j=1}^{n}\sum_{i=1}^{c} (u_{ij})^m d_{ij}^2 + \sum_{i=1}^{n} \lambda_i \left(\sum_{j=1}^{c} u_{ij} - 1\right). \tag{24}$$

According to the extremal problem of functional, one should have

$$\begin{aligned} \frac{\partial L}{\partial u_{ij}} &= 0, \\ \frac{\partial L}{\partial v_i} &= 0. \end{aligned} \tag{25}$$

By solving which, the membership degree and cluster center can be obtained as

$$\begin{aligned} u_{ij} &= \left[\sum_{q=1}^{c} \left(\frac{d_{ij}}{d_{qj}}\right)^{2/m-1}\right]^{-1}, \\ v_i &= \frac{\sum_{j=1}^{n} u_{ij}^m \hat{X}_j}{\sum_{j=1}^{n} u_{ij}^m}. \end{aligned} \tag{26}$$

Finally, the membership and cluster centers are iterated until the results are stable as

$$\max \left|u_{ij}^{(t+1)} - u_{ij}^{(t)}\right| < \varepsilon. \tag{27}$$

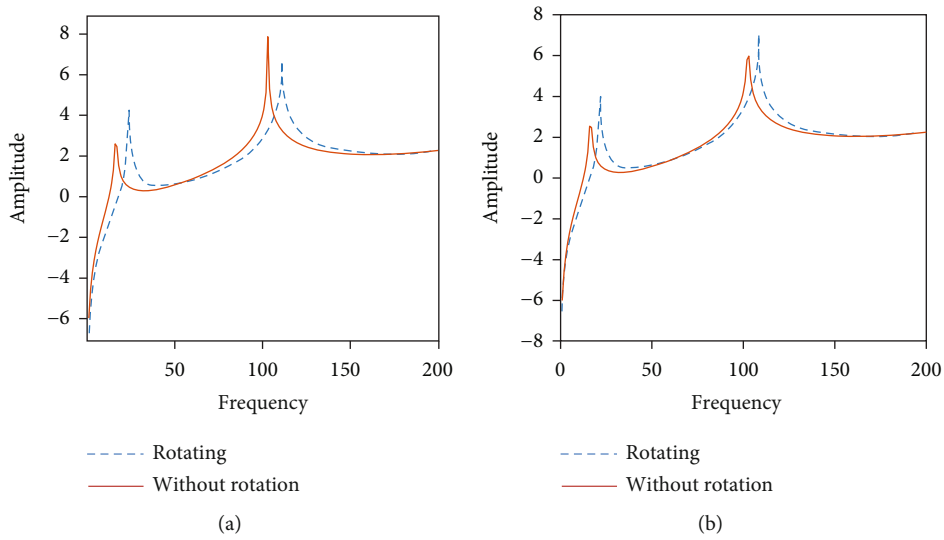

Figure 11: Frequency responses of beams with and without rotation: (a) present results and (b) COMSOL.

3. Results and Discussions

In above, we have talked about the key calculation steps, and here, we will present the flowchart of the key steps in details that can be seen from Figure 2.

Prior to the main topic of this investigation, the verification is carried out by comparing the present vibration behaviors of a damaged beam with those obtained by simulation and experiment. There are two man-made damages on the beam as shown in Figure 3, i.e., a circle pit with a diameter of 0.005 m, and a rectangular notch whose width and depth are 0.002 m and 0.0015 m. The two damages are located at 0.11 m and 0.235 m from the fixed end. The geometrical dimensions and material parameters of the beam are $L = 0.5$ m, $b = 0.025$ m, $h = 0.005$ m, $\rho = 2700\,\text{kg/m}^3$, and $E = 70$ GPa. The equipment and the specimen used in this experiment are shown in Figure 4. Comparisons of natural frequencies of normal and damaged beams between different methods are shown in Table 2, and the frequency responses of the beam are displayed in Figure 5.

It can be noted from the table and figure that both the natural frequencies and frequency responses obtained by the present study agree well with those from the experiment and simulation. Moreover, time-domain responses of the beams with and without damages are computed by the Runge-Kutta method, and the cluster analysis is then carried out using the FCM. The results are shown in Figure 6. It can be seen from the figure that the cluster centers for beams with and without damages can be obtained, and all the vibration signals can be clustered into two categories no matter for the experimental results and the theoretical results, which indicates the correctness and effectiveness of the cluster analysis.

In the above investigation, from the cluster analysis, the damages on the beams are detected. In order to determine the exact positions of the damages, the curvature of frequency response function is applied. The theoretical and simulation results are shown in Figure 7. According to the theory of FRF curvature, the curve of curvature will mutate

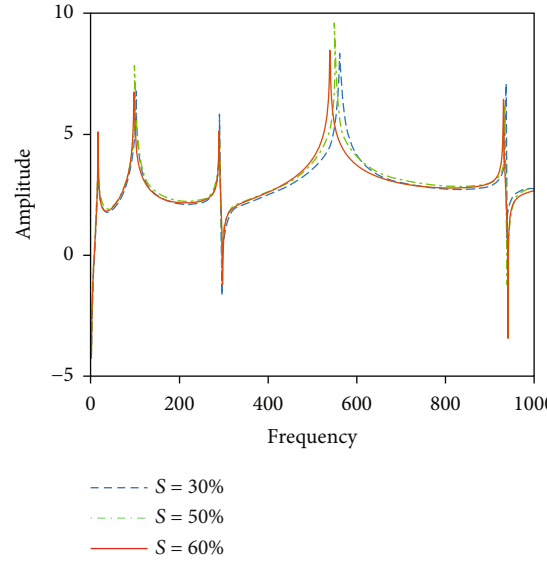

Figure 12: Frequency responses of rotating beams with different damage degrees.

at positions of damage. Judging from Figures 7(a) and 7(b), the damages occur near point 3 and point 6, where the real positions for the two damages can be observed through the schematic diagram (Figure 8). The experimental result is shown in Figure 9. In the experiment, more measuring points are applied. The damage positions determined by the experimental results agree well with those by theoretical analysis and numerical simulation.

The above examples verify the correctness and effectiveness of FCM and curvature of FRF methods. When the rotation of the beam is considered, firstly, the cluster analysis is carried out. Using the FCM, two cluster center of the vibration signals can be obtained, i.e., (0.0101, 0.0059) and (0.0026, 0.0013), as shown in Figure 10, which indicates that damages may occur on the rotating beam.

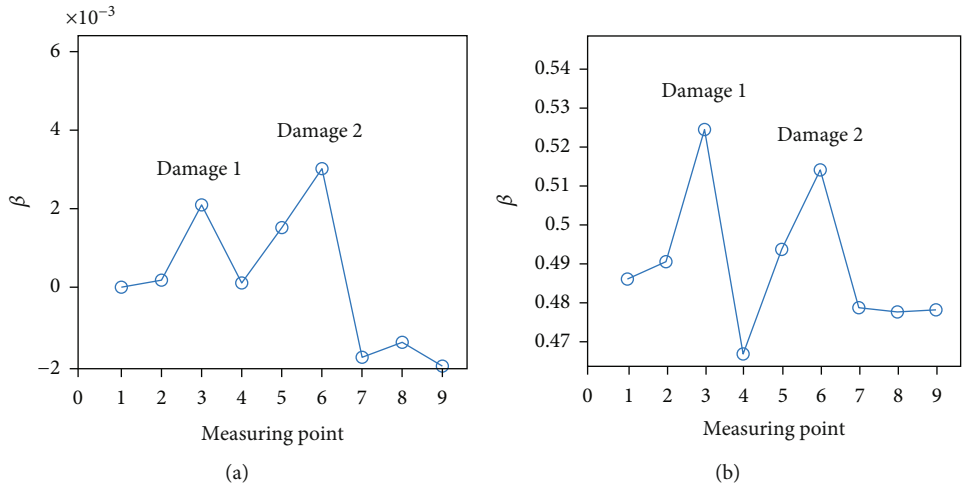

Figure 13: FRF curvature of rotating beam by different methods: (a) present result and (b) COMSOL.

Next, the exact positions of damages on the rotating beam will be determined. Natural frequencies of the rotating beam are calculated and compared with those obtained by COMSOL to verify the correctness of the formulations considering rotation. The results are shown in Table 3. It can be seen from the table that the present results agree well with the simulation results. It is also found that when the rotation is taken into account, the natural frequency increases compared with that of the beam without rotation. This is the stain-stiffening effect due to matrix K_r in Equation (8). The corresponding frequency responses are shown in Figure 11, from which we can get the same conclusion as Table 3 shown.

The influences of the degree of damage on the vibration behaviors are also studied. An index S is introduced here, i.e., $S = h_e/h$, where h_e is the depth of the notch. Three different ratios, i.e., $S = 30\%$, 50%, and 60%, are compared. The frequency responses are shown in Figure 12. It can be noted from the figure that the influences of the damage degree on the lower-order mode are relatively tiny. As for the higher-order modes, the natural frequency decreases with the increase of the damage degree.

The above figure visually illustrates the comparison between numerical calculation and COMSOL solution, further demonstrating the correctness of numerical calculation. It can be seen from the above figure that due to the rotation softening effect, the natural frequency of the structure will increase, causing the image to shift to the right.

At last, the exact positions of damages on the rotating beam are determined by the curvature of FRF. The results obtained by theoretical analysis and numerical simulation are shown in Figure 13. According to the theory of FRF curvature, the curve of curvature will mutate at positions of damage. Judging from Figures 13(a) and 13(b), the damages occur near point 3 and point 6, where the real positions for the two damages are shown in Figure 8.

4. Conclusion

In this paper, damage identification of rotating beams is studied based on FRF curvature and fuzzy C-mean cluster methods. Compared with other article, this article will apply both FRF curvature and fuzzy C-mean cluster methods to damage identification of blade structures. The identification method based on fuzzy C-mean cluster will determine beams in different states, and then, the identification technology based on FRF curvature will determine the damage location of the beams. At the same time, this article successfully identifies and determines the damage location when the model is in rotation. The dynamic model of the rotating beam is constructed by the assumed mode method, and the stress stiffening effect is observed. Theoretical, numerical simulation and experimental studies are carried out to verify the correctness and effectiveness of the present method. The flowing conclusions can be drawn

(1) When damage occurs to the structure, the frequency response curve shows that with the increase of damage to the structure, the stiffness and natural frequency of the structure will decrease gradually

(2) By detecting the time-domain responses of the rotating beam, different states of structure can be separated by FCM-based clustering method

(3) When one or more damage occurs to a structure, the FRF curvature-based identification method can accurately identify the damage locations

(4) The combination of the fuzzy C-mean cluster and the FRF curvature methods are effective in damage identification for rotating blades

5. Prospect

This article modeled the structure of helicopter blades by rotating a cantilever beam and conducts relevant research on damage identification methods based on fuzzy C-mean cluster and the FRF curvature methods. There are some shortcomings in the research, and I hope to solve these problems in the near future:

(1) In the study of cantilever beam simulation in this article, the influence of torsion on the simulation was not considered. The actual rotor model has a torsion angle, and the influence of bending torsion coupling effect on motion should be considered at the beginning of establishing the dynamic model. In addition, there are still some shortcomings in the experimental aspect, and a complete control should be conducted with sufficient and extensive experiments. However, due to the lack of corresponding single damage beams and horizontal rotating turntables, it is impossible to simulate, and there is a lack of comparison results with numerical calculations and simulations

(2) The arrangement of sensors also has shortcomings: in practical engineering applications, a reasonable arrangement of sensors can not only obtain accurate signals but also save some research funds to a certain extent. During the arrangement process, it is often necessary to establish corresponding finite element models and compare them with the actual structure to optimize the arrangement of sensors

(3) The fuzzy C-means cluster method should be an unsupervised machine learning algorithm, but due to insufficient research on cluster method, this research goal has not been achieved, the recognition of fluctuations has certain limitations

Data Availability

Data availability is not applicable to this article as no new data were created or analyzed in this study.

Conflicts of Interest

The authors declare that they have no conflicts of interest.

Acknowledgments

The work described in this paper was supported by grants from the High-Level Oversea Talent Introduction Plan, the National Natural Science Foundation of China (Grant No. 11802069), and the Research Team Project of Heilongjiang Natural Science Foundation (Grant No. TD2020A001).

References

[1] J. Serafini, G. Bernardini, R. Porcelli, and P. Masarati, "In-flight health monitoring of helicopter blades via differential analysis," *Aerospace Science and Technology*, vol. 88, pp. 436–443, 2019.

[2] J. Serafini, G. Bernardini, R. Porcelli, and P. Masarati, "Shape sensing and structural health monitoring of rotor blades from strain analysis," in *American Helicopter Society 73rd Annual Forum*, Fort Worth, USA, 2017.

[3] L. Zhou, T. Q. Zhang, Y. Y. Luo, and Y. Liu, "A new crack detection method based on the correlation analysis of frequency response function curvature differentiation (FRFCD)," *International Journal of Structural Stability and Dynamics*, vol. 22, no. 15, p. 2250177, 2022.

[4] L. H. Manring, J. F. Schultze, S. J. Zimmerman, and B. P. Mann, "Improving magnitude and phase comparison metrics for frequency response functions using cross-correlation and log-frequency shifting," *Journal of Sound and Vibration*, vol. 539, article 117255, 2022.

[5] I. Alshalal, A. Muslim, J. H. Mohmmed, and A. A. Rashed, "Frequency response function curvature technique to detect damage for simply supported beam under harmonic excitation," *AIP Conference Proceedings*, vol. 2386, no. 1, article 040034, 2022.

[6] N. Ayisha, B. Ummul, A. Muhammad, Z. N. Syed, and I. Asif, "Damage detection based on output-only measurements using cepstrum analysis and a baseline-free frequency response function curvature method," *Science Progress*, vol. 105, no. 1, article 003685042110644, 2022.

[7] R. P. C. Sampaio, N. M. M. Maia, and J. M. M. Silva, "Damage detection using the frequency-response-function curvature method," *Journal of Sound and Vibration*, vol. 226, no. 5, pp. 1029–1042, 1999.

[8] N. M. M. Maia, J. M. M. Silva, E. A. M. Almas, and R. P. C. Sampaio, "Damage detection in structures: from mode shape to frequency response function methods," *Mech Systems and Signal Process*, vol. 17, no. 3, pp. 489–498, 2003.

[9] L. V. Palomino, V. Steffen, and R. M. Finzi Neto, "Probabilistic neural network and fuzzy cluster analysis methods applied to impedance-based SHM for damage classification," *Shock and Vibration*, vol. 2014, Article ID 401942, 12 pages, 2014.

[10] Y. Ling, J. H. Zhu, and L. L. Yu, "Structural damage detection in a truss bridge model using fuzzy clustering and measured FRF data reduced by principal component projection," *Advances in Structural Engineering*, vol. 16, no. 1, pp. 207–217, 2013.

[11] H. B. Liu, X. Q. Wang, and Y. Jiao, "Damage identification for irregular-shaped bridge based on fuzzy C-means clustering improved by particle swarm optimization algorithm," *Journal of Vibroengineering*, vol. 18, no. 4, pp. 2149–2166, 2016.

[12] J. S. Huang, K. Y. Zhou, J. L. Xu, K. Wang, and H. W. Song, "Flap-wise vibrations of non-uniform rotating cantilever beams: an investigation with operational experiments," *Journal of Sound and Vibration*, vol. 553, article 117648, 2023.

[13] P. Zhang, H. Qing, and C. F. Gao, "Theoretical analysis for static bending of circular Euler–Bernoulli beam using local and Eringen's nonlocal integral mixed model," *ZAMM-Journal of Applied Mathematics and Mechanics*, vol. 99, no. 8, article e201800329, 2019.

[14] Y. H. Sun, Z. Wang, and Z. G. Song, "Damage identification of rotating beams based on mode parameters and wavelet transform," *Journal of Dynamics and Control*, vol. 21, no. 1, pp. 51–59, 2023.

[15] A. Francois and P. Trompette, "Straight beam models: Hamilton's principle," in *Modelling of Mechanical Systems. Vol. 2*, pp. 130–187, Butterworth-Heinemann, 2005.

[16] H. J. Gao, W. He, Y. H. Song, S. Zhang, and C. Y. Sun, "Modeling and neural network control of a flexible beam with unknown spatiotemporally varying disturbance using assumed mode method," *Neurocomputing*, vol. 314, pp. 458–467, 2018.

[17] Q. Xu, P. Zhang, W. Q. Liu et al., "A platform for fault diagnosis of high-speed train based on big data," *IFAC Papersonline*, vol. 51, no. 18, pp. 309–314, 2018.

[18] X. L. Hou, *Helicopter Transmission System Fault Diagnosis and Health Management Method Based on Big Data*, Xidian University, Dissertation, 2018.

[19] J. S. Chen, D. J. Yu, J. S. Tang, and Y. Yang, "Application of SVM and SVD technique based on EMD to the fault diagnosis of the rotating machinery," *Shock and Vibration*, vol. 16, no. 1, 98 pages, 2009.

[20] L. Xiong, G. Tang, Y. C. Chen, Y. X. Hu, and R. S. Chen, "Color disease spot image segmentation algorithm based on chaotic particle swarm optimization and FCM," *Journal of Supercomputing*, vol. 76, no. 11, pp. 8756–8770, 2020.

[21] L. Guo, L. Chen, X. Lu, and C. L. P. Chen, "Membership affinity lasso for fuzzy clustering," *IEEE Transactions on Fuzzy Systems*, vol. 28, no. 2, pp. 294–307, 2020.

[22] M. Mohammadi and M. Sarmad, "Robustified distance based fuzzy membership function for support vector machine classification," *Iranian Journal of Fuzzy Systems*, vol. 16, no. 6, pp. 191–204, 2019.

[23] M. Kumar and B. Freudenthaler, "Fuzzy membership functional analysis for nonparametric deep models of image features," *IEEE Transactions on Fuzzy Systems*, vol. 28, no. 12, pp. 3345–3359, 2020.

[24] E. H. A. Ruspini, "A new approach to clustering," *Information and Control*, vol. 15, no. 1, pp. 22–32, 1969.

[25] M. S. Yang, K. L. Wu, J. N. Hsieh, and J. Yu, "Alpha-cut implemented fuzzy clustering algorithms and switching regressions," *IEEE Transactions on Systems Man & Cybernetics Part B*, vol. 38, no. 3, pp. 588–603, 2008.

[26] X. L. Sun, Y. G. Zhao, H. L. Wang et al., "Sensitivity of digital soil maps based on FCM to the fuzzy exponent and the number of clusters," *Geoderma*, vol. 171-172, no. 171, pp. 24–34, 2012.

[27] B. Gharnali and S. Alipour, "MRI image segmentation using conditional spatial FCM based on kernel-induced distance measure," *Engineering Technology and Applied Science Research*, vol. 8, no. 3, pp. 2985–2990, 2018.